

Original Article

*Dr Liu, Dr Lencer, and Dr Yang contributed equally to the study.

Cite this article: Liu N, Lencer R, Yang Z, Zhang W, Yang C, Zeng J, Sweeney JA, Gong Q, Lui S (2022). Altered functional synchrony between gray and white matter as a novel indicator of brain system dysconnectivity in schizophrenia. *Psychological Medicine* **52**, 2540–2548. <https://doi.org/10.1017/S0033291720004420>

Received: 19 March 2020
Revised: 11 October 2020
Accepted: 2 November 2020
First published online: 13 January 2021


Key words:

Dysconnectivity; functional activity; functional MRI; gray matter; schizophrenia; white matter

Author for correspondence:

Su Lui, E-mail: lusuwucums@hotmail.com;
Qiyong Gong, E-mail: qygong05@126.com

Altered functional synchrony between gray and white matter as a novel indicator of brain system dysconnectivity in schizophrenia

Naici Liu^{1,*}, Rebekka Lencer^{2,*}, Zhipeng Yang^{3,*}, Wenjing Zhang¹,
Chengmin Yang¹, Jiaxin Zeng¹, John A. Sweeney^{1,4}, Qiyong Gong¹ and Su Lui¹ 

¹Huaxi MR Research Center (HMRRC), Department of Radiology, West China Hospital of Sichuan University, Chengdu, China; ²Department of Psychiatry and Psychotherapy, Otto Creutzfeldt Center for Cognitive and Behavioral Neuroscience, University of Muenster, Muenster, Germany; ³College of Electronic Engineering, Chengdu University of Information Technology, Chengdu, PR, China and ⁴Department of Psychiatry and Behavioral Neuroscience, University of Cincinnati, Cincinnati, OH, USA

Abstract

Background. There is increasing evidence that blood oxygenation level-dependent signaling in white matter (WM) reflects WM functional activity. Whether this activity is altered in schizophrenia remains uncertain, as does whether it is related to established alterations of gray matter (GM) or the microstructure of WM tracts.

Methods. A total of 153 antipsychotic-naïve schizophrenia patients and 153 healthy comparison subjects were assessed by resting-state functional magnetic resonance imaging, diffusion tensor imaging, and high-resolution T1-weighted imaging. We tested for case-control differences in the functional activity of WM, and examined their relation to the functional activity of GM and WM microstructure. The relations between fractional anisotropy (FA) in WM and GM-WM functional synchrony were investigated as well. Then, we examined the associations of identified abnormalities to age, duration of untreated psychosis (DUP), and symptom severity.

Results. Schizophrenia patients displayed reductions of the amplitude of low-frequency fluctuations (ALFF), GM-WM functional synchrony, and FA in widespread regions. Specifically, the genu of corpus callosum not only had weakening in the synchrony of functional activity but also had reduced ALFF and FA. Positive associations were found between FA and functional synchrony in the genu of corpus callosum as well. No significant association was found between identified abnormalities and DUP, and symptom severity.

Conclusions. The widespread weakening in the synchrony of functional activity of GM and WM provided novel evidence for functional alterations in schizophrenia. Regarding the WM function as a component of brain systems and investigating its alternation represent a promising direction for future research.

Introduction

Recent evidence has indicated that the functional activity in white matter (WM) reflected in blood oxygenation level-dependent (BOLD) signals is related to physiological activity in WM fiber tracts (Gawryluk, Mazerolle, & D'Arcy, 2014; Peer, Nitzan, Bick, Levin, & Arzyt, 2017; Wu et al., 2019), and thus may provide a useful biomarker for WM function. This provides a new opportunity to investigate how microstructural alterations in fiber tracts are related to their function, and how alteration in the function of fiber tracts is related to gray matter (GM) function and WM fiber tract integrity.

Whether alterations of the functional activity of WM contribute to the pathophysiology of schizophrenia is yet unclear, as is its relation to GM function and WM fiber integrity (Moskowitz & Heim, 2011). Multiple prior studies document structural alterations in WM integrity in schizophrenia utilizing diffusion tensor imaging (DTI) (Cetin-Karayumak et al., 2019; Meng et al., 2019; Xiao et al., 2018). Most previous studies included chronically ill patients previously treated with antipsychotic medication for years, a factor which has been suggested to exert effects on brain function and both GM and WM structure (Bartzokis et al., 2008; Meng et al., 2019; Xiao et al., 2018).

Mazerolle et al. (2010) and Ding et al. (2018) reported that GM and WM functional networks were activated simultaneously in healthy participants. Altered GM-WM functional connectivity has been reported recently in schizophrenia patients who were taking antipsychotic medication (Jiang et al., 2019) and suggested its foundational value of disruptions in brain connections.

The present cross-sectional study acquired resting-state functional magnetic resonance imaging, DTI, and high-resolution T1-weighted images in a large sample of antipsychotic-naïve schizophrenia patients and healthy comparison subjects. Our aim was to test for alterations in

Table 1. Demographic and clinical characteristics of antipsychotic-naïve schizophrenia patients and healthy comparison subjects

Characteristics	Schizophrenia patients (<i>N</i> = 153)		Healthy comparison subjects (<i>N</i> = 153)		<i>p</i> value
	Mean	s.d.	Mean	s.d.	
Age (years)	27.05	11.39	26.59	9.93	0.708
Education (years)	11.34	3.8	12.68	3.2	<0.05
Duration of untreated psychosis (months)	41.19	88.43			
Age at psychosis onset	23.62	7.64			
Gender					
Female	79		86		0.422
PANSS scores					
Total	90.21	16.77			
Positive symptoms	24.66	6.42			
Negative symptoms	19.37	8.25			
General psychopathology symptoms	46.18	9.34			

BOLD signals in WM tracts, and their temporal synchrony with BOLD signals in GM regions and their relation to fiber tract integrity assessed by using DTI. We also investigated relations between these brain measures and current illness symptom severity and duration of untreated psychosis (DUP).

Methods and materials

Participants

This investigation included 153 antipsychotic-naïve schizophrenia patients recruited from the Psychiatric Outpatient Clinic or the Mental Health Screening Program of West China Hospital. The Nottingham Onset Schedule was used to evaluate DUP based on information provided by patients, family members, and medical records (Norman & Malla, 2001). Clinical diagnoses were established using the Structured Interview for DSM-IV Axis I Disorders (SCID), and the Positive and Negative Syndrome Scale (PANSS) was used to assess current symptom severity. Healthy comparison subjects (*n* = 153) were recruited through advertisements and assessed using the non-patient version of the SCID to confirm lifetime absence of psychotic, mood, and substance use disorders. Healthy comparison subjects with a known history of a psychiatric disorder in their first- or second-degree relatives were excluded. Additional exclusion criteria in both groups included a history of traumatic brain injury, or significant systemic or neurological disorder. All participants were right-handed and of Han ancestry (Table 1). This investigation was approved by the research ethics committee of West China Hospital of Sichuan University. Written informed consent was obtained from all study participants.

MRI data acquisition

All MRI data were collected on the same 3-T scanner (EXCITE, General Electric, Milwaukee). Padding within the head coil limited subject's head motion and earplugs were provided. During scanning, subjects were instructed to relax with eyes closed, without falling asleep or systematic thinking (confirmed by a self-

report of subjects immediately after scans). All scans were reviewed by an experienced neuroradiologist to rule out gross brain abnormalities.

Functional imaging studies used a gradient-echo echo-planar imaging sequence with TR = 2s, TE = 30 ms, flip angle = 90°, 64 × 64 matrix size, and a field of view of 240 × 240 mm² resulting in a voxel size of 3.75 × 3.75 × 5 mm³. Each functional run comprised 200 image volumes and each brain volume contained 30 axial slices with no interslice gap.

DTI data were acquired using a bipolar diffusion-weighted spin-echo echo planar imaging sequence with TR = 1s, TE = 70 ms, and a 128 × 128 matrix over a field of view of 240 × 240 mm resulting in 50 axial slices of 3 mm thickness covering the whole brain without gap. Each DTI data set included 15 images of unique diffusion directions (*b* = 1000 s/mm²) and a non-diffusion image (*b* = 0).

For registration purposes, high-resolution anatomical T1-weighted images were acquired with a three-dimensional spoiled gradient sequence: TR = 8.5 ms, TE = 3.5 ms, TI = 400 ms, flip angle = 12°, with a 240 × 240 matrix over a field of view of 240 × 240 mm resulting in 156 axial slices of 1 mm thickness.

It was confirmed that all study participants did not have head translation movements >2 mm or rotations >2°.

Functional data preprocessing

The BOLD image preprocessing was carried out using Statistical Parametric Mapping software (SPM12). The analysis pipeline was in accordance with one reported previously (Ding et al., 2018). The main procedures were as follows:

First, the first five volumes of each scan were discarded to allow for T1 equilibration. Second, the remaining functional images were slice-time corrected and realigned using a six-parameter (rigid-body 6) linear transformation. In order to reduce the effects of head motion and non-neuronal BOLD fluctuations, the Friston's 24-parameter model (Friston, Williams, Howard, Frackowiak, & Turner, 1996) was included as a covariate in image analysis. Third, T1-weighted images were segmented into GM, WM, and cerebrospinal fluid and registered to the mean BOLD image. After that, images were normalized into

Table 2. Differences in the amplitude of low-frequency fluctuation (ALFF) at voxel-level in white matter (WM) between antipsychotic-naïve schizophrenia patients and healthy comparison subjects

	ALFF alteration in WM	Cluster size	Peak coordinate			T value	Corrected p value
			X	Y	Z		
HC > P	Genu of corpus callosum	213	3	18	3	4.250	0.007
	Splenium of corpus callosum	31	12	-33	30	3.900	0.010
	Anterior corona radiata R	72	21	21	15	3.860	0.011
	Cingulum (cingulate gyrus) R	30	9	30	18	4.130	0.007

HC, healthy comparison subjects; P, antipsychotic-naïve schizophrenia patients.

Montreal Neurological Institute (MNI) space, each voxel was resampled to $3 \times 3 \times 3 \text{ mm}^3$. Slow signal drift and physiological noise in BOLD images were removed by temporal band-pass filtering within 0.01–0.1 Hz.

The amplitude of low-frequency fluctuations (ALFF) of each WM bundle and GM region was obtained from the averaged time series within each region of interest (ROI).

Functional synchrony analyses

The GM and WM masks were separated into 84 regions (GM) and 48 tracts (WM), respectively, by applying the PickAtlas tool (Maldjian, Laurienti, Kraft, & Burdette, 2003) based on Brodmann's areas and the JHU ICBM-DTI-81 WM atlas (Mori et al., 2008). To avoid confounds of signal corruption by neighboring GM and vascular structures, the WM mask threshold was set at a high value of 0.80. Mean time series were constructed by averaging BOLD signals in voxels of every GM region and WM tract before conducting pairwise correlation analyses between WM tracts and GM regions. The correlation coefficients of BOLD signals in pairwise WM bundle and GM region were assessed by Pearson correlation analysis. The functional correlation or synchrony was adopted as a brain measure and reflected by the correlation coefficients. In this study, the functional correlation or synchrony was used to reveal the synchronous degree of BOLD signals in WM tracts and neural activity within GM regions.

Diffusion data preprocessing

Routine DTI preprocessing was performed with the Full Pipeline of the Pipeline for Analyzing Brain Diffusion Images toolkit (PANDA), including head motion and eddy current correction. Then, non-linear registration was used to register the individual fractional anisotropy (FA) map into MNI space. Finally, the atlas-based analysis was performed by calculating the regional averages of voxels in the transformed FA map according to the JHU ICBM-DTI-81 WM atlas (Mori et al., 2008).

Statistical analyses of brain measures

The group differences of ALFF in WM ROIs, and correlation coefficients of BOLD signals in pairwise WM bundle and GM region, and FA were identified using analysis of covariance (ANCOVA) in SPSS (Statistical Product and Service Solutions for Windows version 24.0) with age and gender as covariates. Bonferroni correction was used to correct for multiple comparisons in all analyses.

For exploratory purposes, comparison of schizophrenia patients and healthy comparison subjects in voxel-based ALFF maps was performed using ANCOVA in SPM12 software with age and gender as covariates. A minimum cluster size of 20 contiguous voxels preserved cluster significance at $p < 0.05$, FDR-corrected.

Partial correlation analyses between FA and ALFF, and GM–WM correlation coefficients

For patient group, the associations of FA to ALFF, and GM–WM correlation coefficients were assessed in WM regions with significant group differences by partial correlation analyses with age and gender as covariates. Bonferroni correction was used to correct for multiple comparisons.

Partial correlation analyses between brain measures and age, DUP, symptom severity

Partial correlation analyses were performed between brain measures that showed significant group differences and age, and DUP, and symptom severity scores. Age and gender were covariates in the analyses of DUP and symptom correlations, and gender was a covariate in the analyses of age effects. Bonferroni correction was used to correct for multiple comparisons.

Results

Group differences of WM function

In exploratory analyses, compared to healthy comparison subjects, schizophrenia patients showed lower ALFF at voxel-level in the genu and splenium of corpus callosum, right anterior corona radiata, and right cingulum (cingulate gyrus) ($p < 0.05$, FDR-corrected, Table 2).

Though, we found no significant group differences in ALFF in 48 WM ROIs.

Group differences of functional correlations between GM regions and WM tracts

The maps shown in Fig. 1 represent correlations between function in WM tracts with that in GM regions, reflecting GM–WM functional synchrony. The horizontal and vertical stripes shown in Fig. 1a, b reflect the synchronous BOLD responses within distinct pairs of WM tracts and GM regions.

Compared to healthy comparison subjects, schizophrenia patients showed weaker GM–WM functional correlations in widespread regions (p values were thresholded at a Bonferroni-

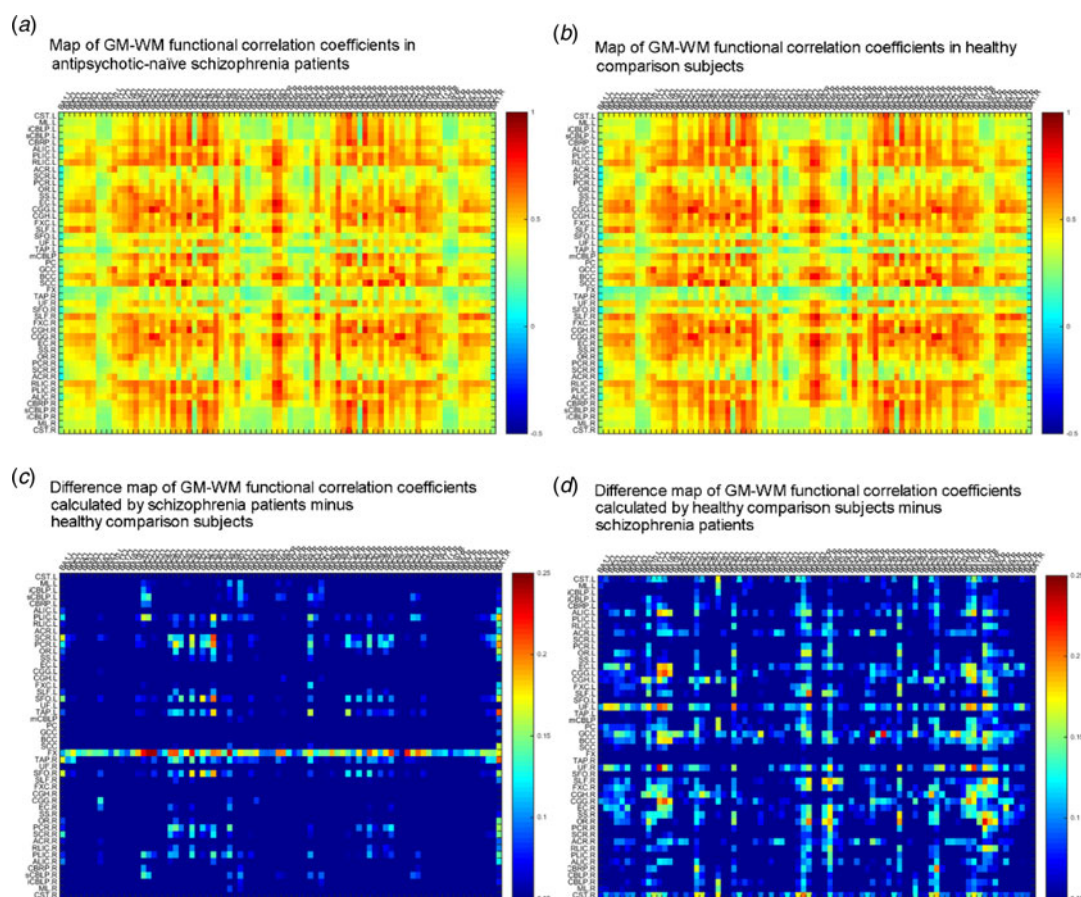


Fig. 1. (a–d) Blood oxygenation level-dependent (BOLD) signals reflecting temporal correlations between gray matter (GM) regions and white matter (WM) tracts in antipsychotic-naïve schizophrenia patients (a), in healthy comparison subjects (b), and group differences of GM–WM functional correlation coefficients (c, d). Greater GM–WM functional correlation coefficients in schizophrenia patients compared to healthy comparison subjects (c) and greater GM–WM functional correlation coefficients in healthy comparison subjects compared to schizophrenia patients (d) are indicated by red/warm color, and lower functional correlation coefficients are indicated by blue/cold color. BA indicates Brodmann area. List of abbreviations and full names for WM tracts: CST, corticospinal tract; ML, medial lemniscus; iCBLP, inferior cerebellar peduncle; sCBLP, superior cerebellar peduncle; CBRP, cerebral peduncle; ALIC, anterior limb of internal capsule; PLIC, posterior limb of internal capsule; RLIC, retrolenticular part of internal capsule; ACR, anterior corona radiata; SCR, superior corona radiata; PCR, posterior corona radiata; OR, optic radiation; SS, sagittal stratum; EC, external capsule; CCG, cingulum (cingulate gyrus); CGH, cingulum (hippocampus); FXC, fornix (cres); SLF, superior longitudinal fasciculus; SFO, superior fronto-occipital fasciculus; UF, uncinate fasciculus; TAP, tapetum; mCBLP, middle cerebellar peduncle; PC, pontine crossing tract; GCC, genu of corpus callosum; BCC, body of corpus callosum; SCC, splenium of corpus callosum; FX, fornix (body).

corrected threshold of $p < 0.05/82 = 0.0006$, Table 3, Fig. 2) including corpus callosum (genu and body), bilateral external capsule, bilateral cingulum, bilateral uncinate fasciculus, bilateral superior longitudinal fasciculus, right sagittal stratum, right cerebral peduncle, right posterior thalamic radiation, left anterior limb of internal capsule with diffuse cortical regions including visual cortex, cingulate cortex, temporal cortex, prefrontal cortex, pars orbitalis, and premotor cortex. Stronger GM–WM functional correlations were observed between fornix (column and body) and temporal cortex, piriform cortex, and angular gyrus in patients compared to healthy comparison subjects.

Group differences of WM structure

Regarding the integrity of WM structure, schizophrenia patients showed reduced FA in widespread tracts (p values were thresholded at a Bonferroni-corrected threshold of $p < 0.05/48 = 0.001$, Table 4), including bilateral anterior corona radiata, bilateral cerebral peduncle, corpus callosum, right cingulum (cingulate gyrus and hippocampus), and right fornix(crus)/stria terminalis.

Relations between FA and ALFF, and GM–WM correlation coefficients

In patients, positive associations were found between FA in the genu of corpus callosum and GM–WM correlation coefficients for the association between the genu of corpus callosum and bilateral pars orbitalis (part of the inferior frontal gyrus), and right anterior prefrontal cortex ($p < 0.05$, uncorrected). Though, we found no significant associations between FA and ALFF neither at voxel-level nor by the ROI analyses.

Relations between brain measures and age, DUP, and symptom severity

In patients, regression analyses revealed a positive linear relationship between age and GM–WM correlation coefficients for the association between the left external capsule and visual cortex ($p < 0.05$, uncorrected, online Supplementary Fig. S1, Table S1). FA values in the genu of corpus callosum showed a negative association with age in schizophrenia patients ($p < 0.05$, uncorrected, online Supplementary Fig. S2, Table S2). No significant age-related

Table 3. Differences in gray matter (GM)-white matter (WM) correlation coefficients between antipsychotic-naïve schizophrenia patients and healthy comparison subjects

	WM tract	GM region	Schizophrenia patients		Healthy comparison subjects		F value	p value
			Mean	s.d.	Mean	s.d.		
HC > P	Cerebral peduncle R	Ventral anterior cingulate cortex R	0.487	0.203	0.567	0.168	14.539	0.00017
	Anterior limb of internal capsule L	Pars orbitalis, part of the inferior frontal gyrus L	0.558	0.150	0.619	0.139	13.287	0.00032
		Ventral anterior cingulate cortex L	0.595	0.152	0.652	0.132	13.039	0.00036
	Posterior thalamic radiation R	Anterior prefrontal cortex R	0.346	0.210	0.436	0.206	14.256	0.00019
		Dorsolateral prefrontal cortex R	0.402	0.177	0.478	0.172	15.128	0.00012
		Pars orbitalis, part of the inferior frontal gyrus L	0.398	0.180	0.477	0.198	14.226	0.00020
	Sagittal stratum R	Dorsolateral prefrontal cortex R	0.444	0.173	0.512	0.151	13.265	0.00032
	External capsule L	Primary visual cortex (V1) L	0.487	0.165	0.560	0.162	16.593	0.00006
		Primary visual cortex (V1) R	0.473	0.168	0.535	0.157	12.224	0.00054
		Secondary visual cortex (V2) L	0.517	0.177	0.593	0.156	16.575	0.00006
		Secondary visual cortex (V2) R	0.509	0.171	0.575	0.156	13.564	0.00027
		Associative visual cortex (V3, V4, V5) L	0.580	0.165	0.646	0.135	15.390	0.00011
		Associative visual cortex (V3, V4, V5) R	0.553	0.153	0.609	0.133	12.183	0.00056
		Premotor and supplementary motor cortex L	0.618	0.149	0.679	0.117	15.761	0.00009
		Premotor and supplementary motor cortex R	0.603	0.153	0.659	0.127	12.060	0.00059
		Ventral anterior cingulate cortex. L	0.667	0.123	0.717	0.108	14.163	0.00020
		Dorsolateral prefrontal cortex L	0.551	0.140	0.607	0.133	12.119	0.00057
	External capsule R	Premotor and supplementary motor cortex R	0.625	0.153	0.692	0.116	18.245	0.00003
		Dorsolateral prefrontal cortex R	0.524	0.168	0.594	0.148	14.280	0.00019
	Cingulum (cingulate gyrus) L	Primary visual cortex (V1) L	0.526	0.164	0.605	0.166	18.232	0.00003
		Primary visual cortex (V1) R	0.539	0.158	0.607	0.154	14.958	0.00014
		Secondary visual cortex (V2) L	0.547	0.186	0.632	0.149	19.730	0.00001
		Secondary visual cortex (V2) R	0.550	0.170	0.621	0.149	15.649	0.00010
		Associative visual cortex (V3, V4, V5) L	0.596	0.180	0.669	0.134	15.948	0.00008
	Cingulum (cingulate gyrus) R	Primary visual cortex (V1) L	0.520	0.175	0.596	0.177	14.580	0.00016
		Primary visual cortex (V1) R	0.536	0.165	0.603	0.160	13.742	0.00025
		Secondary visual cortex (V2) L	0.545	0.188	0.629	0.157	17.776	0.00003
		Secondary visual cortex (V2) R	0.540	0.170	0.618	0.155	17.729	0.00003
		Associative visual cortex (V3, V4, V5) L	0.595	0.185	0.666	0.144	13.711	0.00025
		Associative visual cortex (V3, V4, V5) R	0.582	0.147	0.642	0.138	12.914	0.00038
	Cingulum (hippocampus) L	Primary visual cortex (V1) L	0.550	0.158	0.617	0.154	14.176	0.00020
		Primary visual cortex (V1) R	0.563	0.166	0.635	0.141	16.540	0.00006
		Ectosplenial portion of the retrosplenial region L	0.519	0.169	0.584	0.128	14.557	0.00017
	Cingulum (hippocampus) R	Primary visual cortex (V1) L	0.563	0.152	0.626	0.153	13.513	0.00028
		Primary visual cortex (V1) R	0.587	0.157	0.658	0.129	18.124	0.00003
		Secondary visual cortex (V2) R	0.591	0.154	0.650	0.138	12.723	0.00042

(Continued)

Table 3. (Continued.)

WM tract	GM region	Schizophrenia patients		Healthy comparison subjects		F value	p value	
		Mean	s.d.	Mean	s.d.			
	Subgenual area R	0.566	0.203	0.641	0.147	13.402	0.00030	
	Ectosplenial portion of the retrosplenial region L	0.514	0.145	0.570	0.127	12.705	0.00042	
Superior longitudinal fasciculus L	Pars orbitalis, part of the inferior frontal gyrus L	0.526	0.165	0.607	0.163	19.081	0.00002	
Superior longitudinal fasciculus R	Dorsolateral prefrontal cortex R	0.518	0.167	0.594	0.160	16.444	0.00006	
Uncinate fasciculus L	Primary visual cortex (V1) L	0.388	0.166	0.473	0.196	17.574	0.00004	
	Primary visual cortex (V1) R	0.402	0.163	0.477	0.179	15.562	0.00010	
	Secondary visual cortex (V2) L	0.427	0.176	0.506	0.191	14.622	0.00016	
	Secondary visual cortex (V2) R	0.425	0.173	0.504	0.182	15.544	0.00010	
Uncinate fasciculus R	Primary visual cortex (V1) L	0.383	0.161	0.482	0.185	24.661	0.00001	
	Primary visual cortex (V1) R	0.402	0.159	0.493	0.168	23.372	0.00001	
	Secondary visual cortex (V2) L	0.435	0.166	0.506	0.187	12.423	0.00049	
	Secondary visual cortex (V2) R	0.433	0.162	0.507	0.172	14.882	0.00014	
Genu of corpus callosum	Ventral posterior cingulate cortex R	0.472	0.177	0.545	0.168	13.016	0.00036	
	Anterior prefrontal cortex R	0.532	0.174	0.596	0.141	12.696	0.00043	
	Pars orbitalis, part of the inferior frontal gyrus L	0.540	0.155	0.603	0.137	14.431	0.00018	
	Pars orbitalis, part of the inferior frontal gyrus R	0.588	0.149	0.643	0.128	12.212	0.00055	
	Ectorhinal area, now part of the perirhinal cortex R	0.339	0.247	0.427	0.195	12.223	0.00054	
	Inferior temporal gyrus R	0.532	0.190	0.609	0.150	14.979	0.00013	
	Middle temporal gyrus R	0.417	0.176	0.484	0.150	13.378	0.00030	
	Temporopolar area R	0.420	0.215	0.524	0.167	21.940	0.00001	
	Ventral anterior cingulate cortex. L	0.533	0.149	0.591	0.123	14.405	0.00018	
	Body of corpus callosum	Secondary visual cortex (V2) L	0.527	0.197	0.599	0.158	12.530	0.00046
Associative visual cortex (V3, V4, V5) L		0.577	0.203	0.648	0.145	12.543	0.00046	
P > HC	Column and body of fornix	Angular gyrus, may be part of Wernicke L	0.286	0.196	0.190	0.206	17.280	0.00004
		Superior temporal gyrus L	0.277	0.223	0.181	0.229	13.537	0.00028
		Middle temporal gyrus L	0.310	0.204	0.220	0.227	13.135	0.00034
		Piriform cortex L	0.518	0.182	0.430	0.240	12.711	0.00042

HC, healthy comparison subjects; P, antipsychotic-naïve schizophrenia patients.

associations were observed with brain measures in healthy comparison subjects. No significant associations were found between DUP and brain measures in schizophrenia patients.

Regarding the associations between symptom severity and brain measures in the patient group, we observed no significant associations between them.

Discussion

The main purpose of this study was to identify the alterations of functional activity in WM and to examine its relationship to the

alterations of functional activity in GM and microstructural WM integrity in schizophrenia patients independently from possible confounds by antipsychotic medication. These aspects have not been reported in depth before. We identified widespread weakening in the synchrony of functional activity of GM and WM in patients, especially between WM tracts connecting fronto-temporal regions, interhemispheric homologous regions, cortico-subcortical circuits, and visual, cingulate, temporal, prefrontal cortex.

Based on the idea that synchronization between GM and WM functional activity in brain systems reflect how well distinct cortical areas are able to communicate with each other through

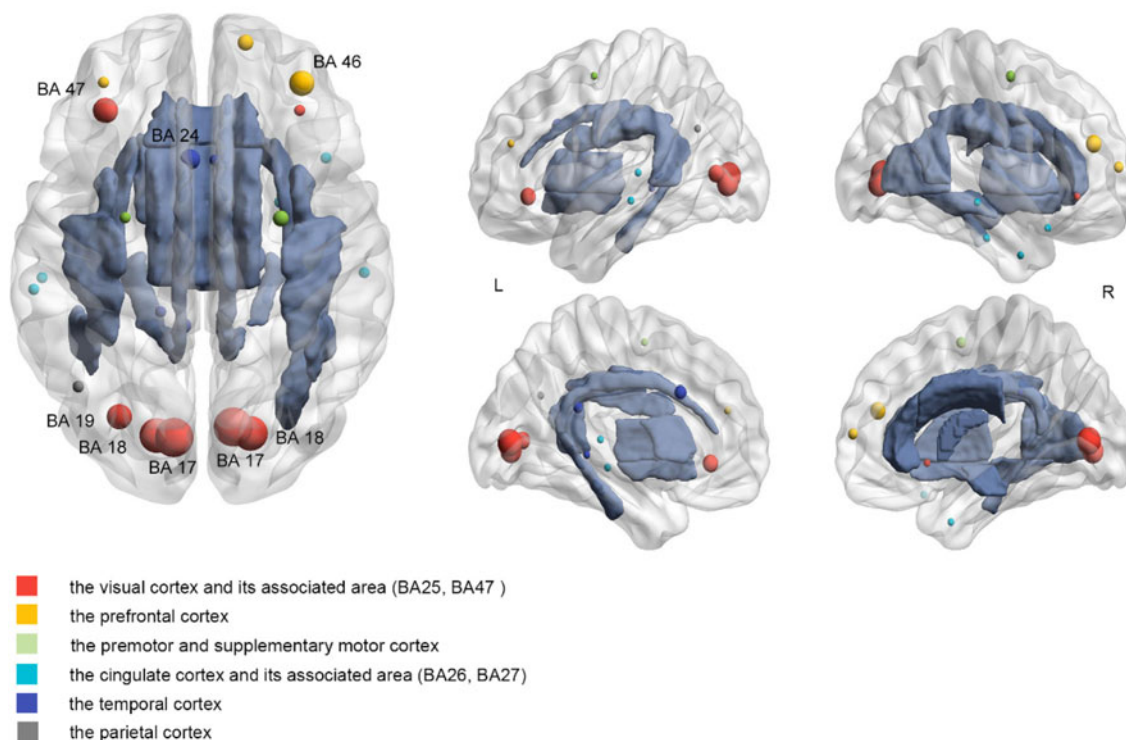


Fig. 2. Differences in gray matter (GM)-white matter (WM) functional correlation coefficients between antipsychotic-naïve schizophrenia patients and healthy comparison subjects. Shown are GM regions and WM tracts for which significant group differences in GM-WM functional correlations were identified. The nodes denote GM regions with their size indicating the frequency of significant correlations with WM tracts. GM regions were labeled if at least three or more correlations were identified. BA indicates Brodmann area. R, right; L, left.

Table 4. Differences in fractional anisotropy (FA) between antipsychotic-naïve schizophrenia patients and healthy comparison subjects

		Schizophrenia patients		Healthy comparison subjects		<i>F</i> values	<i>p</i> value
		Mean	s.d.	Mean	s.d.		
HC > P	Anterior corona radiata R	0.431	0.023	0.444	0.026	20.254	0.00001
	Anterior corona radiata L	0.432	0.026	0.443	0.025	13.008	0.00037
	Cerebral peduncle R	0.637	0.023	0.649	0.023	19.370	0.00002
	Cerebral peduncle L	0.642	0.022	0.652	0.023	12.940	0.00038
	Cingulum (cingulate gyrus) R	0.389	0.025	0.402	0.025	17.597	0.00004
	Cingulum (hippocampus) R	0.379	0.029	0.392	0.028	14.728	0.00016
	Genu of corpus callosum	0.588	0.024	0.597	0.020	11.328	0.00088
	Body of corpus callosum	0.533	0.029	0.543	0.026	10.159	0.00096
	Splenium of corpus callosum	0.637	0.019	0.644	0.017	10.610	0.00093
	Fornix (crus)/stria terminalis R	0.498	0.029	0.510	0.030	12.447	0.00049

HC, healthy comparison subjects; P, antipsychotic-naïve schizophrenia patients.

the dense WM fiber network. The widespread weakening of GM-WM functional correlations in schizophrenia patients is consistent with the concept of schizophrenia as a dysconnectivity syndrome. Previous studies reported that BOLD signal changes in WM are related to BOLD signal changes in GM during task-based fMRI, indicating that altered BOLD signals in WM may contribute to behaviorally-relevant alterations of neural activity in brain GM (Gawryluk *et al.*, 2014).

Though disruptions of functional correlations in WM tracts were widespread in the present study, their association with alterations in GM regions was mainly distributed in the visual cortex, prefrontal cortex, cingulate cortex, and temporal cortex. Alterations in these GM regions are believed to play important roles in the pathophysiology of schizophrenia. For instance, anterior and posterior cingulate cortex are components of the default mode network that is altered in schizophrenia (Li *et al.*, 2019;

Lui et al., 2015). Deficits in executive function, attention, and working memory have been linked to dysfunction of the dorsolateral prefrontal cortex (Chechko et al., 2018; Lencer et al., 2019); and there are multiple imaging and psychophysical studies showing visual cortex alterations in schizophrenia.

Peer et al. (2017) reported the WM functional networks were related to distributed GM networks in healthy individuals in areas including the default-mode, dorsal attention, and frontoparietal control networks. Thus, our findings suggest a role for functional disruptions of WM tracts in schizophrenia with implications for alterations of communication between distant GM regions reflected in the relatively weak spatial coherence GM and WM function.

While there were anatomic dissociations between regional structural and functional alternations as has been reported previously (Liu et al., 2019), there were also anatomic associations of GM and WM function and WM microstructure. The altered connections were found between WM tracts with disrupted structural integrity (e.g. corpus callosum, cingulum) and the GM regions with disrupted functional synchrony (e.g. the prefrontal cortex, visual cortex, temporal gyri, cingulate cortex) in schizophrenia patients. Moreover, both reduced ALFF and FA were observed in the genu and splenium of corpus callosum, right anterior corona radiata, right cingulum (cingulate gyrus) in schizophrenia patients when compared to healthy comparison subjects despite some regional inconsistencies between regional patterns of structural and WM functional correlations.

Right cerebral peduncle, right cingulum, and genu of corpus callosum also demonstrated disruptions in structural integrity and weakening functional synchrony with GM regions to which they project. Based on these findings, our results suggest that disrupted WM integrity might provide the structural basis for the alternations of WM functional measures and the ability of WM to support the functional integration of GM regions to support cognition and behavior. Although our findings showed partially spatial overlapping in altered WM function and fiber tract integrity which was known to be impaired in schizophrenia (Skudlarski et al., 2010), we found no significant correlations between ALFF and FA in WM. This might reflect the independence of WM functional activity from WM structural integrity as a novel indicator to reveal the pathophysiology of schizophrenia.

Limitations

There are limitations to this study that should be considered when interpreting the results. First, the majority of patients were young adults with a recent onset of schizophrenia (Flynn et al., 2003) while the proportion of chronically ill patients was relatively small. This might have resulted in a bias affecting the age and illness-duration-related alternations in functional correlations in patients. However, the age range in the healthy comparison subject group was similar to that in the patient group and no association with age was observed making a possible sample bias unlikely. Second, subcortical and cerebellar regions were not included in the GM atlas employed; therefore, disruption of GM–WM synchrony involving those areas remains to be determined. Third, with smaller volume, the slight movement of patients might affect the detection of BOLD signals in WM. However, the head movement was integrated with a conservative criterion of 2 mm in this study. Fourth, the neurophysiological basis of the BOLD signal changes in WM is still a matter of debate. More clinical and preclinical investigation is required to fully understand the disease and

behavioral significance of alterations in WM function in schizophrenia. Last, the hemodynamic response function in specific WM regions may vary, and impact sensitivity of measured BOLD signal changes to neural activity in WM (Gawryluk et al., 2014). Other technical factors related to this may impact our findings, such as activations arising from neighboring GM and vascular structure impacting BOLD signals of WM pathways related to partial volume effects (Jiang et al., 2019).

Conclusion

Findings from the present study extend knowledge about functional alterations in brain WM in schizophrenia independently from antipsychotic medication or course of illness effects. Our findings provide new information about the model of schizophrenia as a dysconnectivity syndrome reflected in disruptions of the synchrony between GM and WM function. The specific patterns of altered functional synchrony observed in this study might contribute to the pathophysiology of schizophrenia and highlighted the novelty of GM–WM functional correlation as the indicator to investigate the brain function.

Supplementary material. The supplementary material for this article can be found at <https://doi.org/10.1017/S0033291720004420>

Acknowledgements. Dr Su Lui acknowledges the support from Humboldt Foundation's Friedrich Wilhelm Bessel Research Award. This study was supported by the National Natural Science Foundation of China (Project Nos. 81671664 and 81621003, 81820108018, 81901828), National Program for Support of Top-notch Young Professionals (Project No. W02070140), Fundamental Research Funds for the Central Universities (Project No. 2018SCUH0011), Science and Technology Project of the Health Commission of Sichuan Province (Project No. 18ZD035), Sichuan Science and Technology Program (Project No. 2019YJ0155), and 1.3.5 Project for Disciplines of Excellence, West China Hospital, Sichuan University (Project Nos. ZYYC08001 and ZYJC18020). Drs Su Lui and Qiyong Gong contributed equally as senior authors.

Conflict of interest. Dr Sweeney and Dr Zhang consult to VeraSci. Other authors declare no conflicts.

References

- Bartzokis, G., Lu, P. H., Nuechterlein, K. H., Gitlin, M., Doi, C., Edwards, N., ... Mintz, J. (2008). Differential effects of typical and atypical antipsychotics on brain myelination in schizophrenia (vol 93, pg 13, 2007). *Schizophrenia Research*, 99(1–3), 379. doi: 10.1016/j.schres.2007.09.023
- Cetin-Karayumak, S., Di Biase, M. A., Chunga, N., Reid, B., Somes, N., Lyall, A. E., ... Kubicki, M. (2019). White matter abnormalities across the lifespan of schizophrenia: A harmonized multi-site diffusion MRI study. *Molecular Psychiatry*, 25(12), 3208–3219. doi: 10.1038/s41380-019-0509-y
- Chechko, N., Cieslik, E. C., Muller, V. I., Nickl-Jockschat, T., Derntl, B., Kogler, L., ... Eickhoff, S. B. (2018). Differential resting-state connectivity patterns of the right anterior and posterior dorsolateral prefrontal cortices (DLPFC) in schizophrenia. *Frontiers in Psychiatry*, 9, 211. doi: 10.3389/fpsy.2018.00211
- Ding, Z. H., Huang, Y. L., Bailey, S. K., Gao, Y. R., Cutting, L. E., Rogers, B. P., ... Gore, J. C. (2018). Detection of synchronous brain activity in white matter tracts at rest and under functional loading. *Proceedings of the National Academy of Sciences of the USA*, 115(3), 595–600. doi: 10.1073/pnas.1711567115
- Flynn, S. W., Lang, D. J., Mackay, A. L., Goghari, V., Vavasour, I. M., Whittall, K. P., ... Honer, W. G. (2003). Abnormalities of myelination in schizophrenia detected in vivo with MRI, and post-mortem with analysis of oligodendrocyte proteins. *Molecular Psychiatry*, 8(9), 811–820. doi: 10.1038/sj.mp.4001337

- Friston, K. J., Williams, S., Howard, R., Frackowiak, R. S. J., & Turner, R. (1996). Movement-related effects in fMRI time-series. *Magnetic Resonance in Medicine*, 35(3), 346–355. doi: DOI 10.1002/mrm.1910350312
- Gawryluk, J. R., Mazerolle, E. L., & D'Arcy, R. C. N. (2014). Does functional MRI detect activation in white matter? A review of emerging evidence, issues, and future directions. *Frontiers in Neuroscience*, 8. doi: ARTN 23910.3389/fnins.2014.00239
- Jiang, Y. C., Luo, C., Li, X., Li, Y. J., Yang, H., Li, J. F., ... Yao, D. Z. (2019). White-matter functional networks changes in patients with schizophrenia. *Neuroimage*, 190, 172–181. doi: 10.1016/j.neuroimage.2018.04.018
- Lencer, R., Yao, L., Reilly, J. L., Keedy, S. K., McDowell, J. E., Keshavan, M. S., ... Sweeney, J. A. (2019). Alterations in intrinsic fronto-thalamo-parietal connectivity are associated with cognitive control deficits in psychotic disorders. *Human Brain Mapping*, 40(1), 163–174. doi: 10.1002/hbm.24362
- Li, S. Y., Hu, N., Zhang, W. J., Tao, B., Dai, J., Gong, Y., ... Lui, S. (2019). Dysconnectivity of multiple brain networks in schizophrenia: A meta-analysis of resting-state functional connectivity. *Frontiers in Psychiatry*, 10.
- Liu, J. K., Yao, L., Zhang, W. J., Deng, W., Xiao, Y., Li, F., ... Lui, S. (2019). Dissociation of fractional anisotropy and resting-state functional connectivity alterations in antipsychotic-naive first-episode schizophrenia. *Schizophrenia Research*, 204, 230–237. doi: 10.1016/j.schres.2018.08.005
- Lui, S., Yao, L., Xiao, Y., Keedy, S. K., Reilly, J. L., Keefe, R. S., ... Sweeney, J. A. (2015). Resting-state brain function in schizophrenia and psychotic bipolar probands and their first-degree relatives. *Psychological Medicine*, 45(1), 97–108. doi: 10.1017/S003329171400110x
- Maldjian, J. A., Laurienti, P. J., Kraft, R. A., & Burdette, J. H. (2003). An automated method for neuroanatomic and cytoarchitectonic atlas-based interrogation of fMRI data sets. *Neuroimage*, 19(3), 1233–1239. doi: 10.1016/S1053-8119(03)00169-1
- Mazerolle, E. L., Beyea, S. D., Gawryluk, J. R., Brewer, K. D., Bowen, C. V., & D'Arcy, R. C. N. (2010). Confirming white matter fMRI activation in the corpus callosum: Co-localization with DTI tractography. *Neuroimage*, 50(2), 616–621. doi: 10.1016/j.neuroimage.2009.12.102
- Meng, L., Li, K., Li, W., Xiao, Y., Lui, S., Sweeney, J. A., & Gong, Q. (2019). Widespread white-matter microstructure integrity reduction in first-episode schizophrenia patients after acute antipsychotic treatment. *Schizophrenia Research*, 204, 238–244. doi: 10.1016/j.schres.2018.08.021
- Mori, S., Oishi, K., Jiang, H. Y., Jiang, L., Li, X., Akhter, K., ... Mazziotta, J. (2008). Stereotaxic white matter atlas based on diffusion tensor imaging in an ICBM template. *Neuroimage*, 40(2), 570–582.
- Moskowitz, A., & Heim, G. (2011). Eugen Bleuler's Dementia praecox or the group of schizophrenias (1911): A centenary appreciation and reconsideration. *Schizophrenia Bulletin*, 37(3), 471–479. doi: 10.1093/schbul/sbr016
- Norman, R. M. G., & Malla, A. K. (2001). Duration of untreated psychosis: A critical examination of the concept and its importance. *Psychological Medicine*, 31(3), 381–400.
- Peer, M., Nitzan, M., Bick, A. S., Levin, N., & Arzyt, S. (2017). Evidence for functional networks within the human brain's white matter. *Journal of Neuroscience*, 37(27), 6394–6407. doi: 10.1523/Jneurosci.3872-16.2017
- Skudlarski, P., Jagannathan, K., Anderson, K., Stevens, M. C., Calhoun, V. D., Skudlarska, B. A., & Pearlson, G. (2010). Brain connectivity is not only lower but different in schizophrenia: A combined anatomical and functional approach. *Biological Psychiatry*, 68(1), 61–69. doi: 10.1016/j.biopsych.2010.03.035
- Wu, T. L., Wang, F., Li, M. W., Schilling, K. G., Gao, Y. R., Anderson, A. W., ... Gore, J. C. (2019). Resting-state white matter-cortical connectivity in non-human primate brain. *Neuroimage*, 184, 45–55. doi: 10.1016/j.neuroimage.2018.09.021
- Xiao, Y., Sun, H. Q., Shi, S. L., Jiang, D., Tao, B., Zhao, Y. J., ... Lui, S. (2018). White matter abnormalities in never-treated patients with long-term schizophrenia. *American Journal of Psychiatry*, 175(11), 1129–1136.